

Extreme jet distortions in low-*z* radio galaxies

Mark Birkinshaw¹ Josie Rawes² and Diana Worrall³

¹HH Wills Physics Laboratory, University of Bristol,
Tyndall Avenue, Bristol BS8 1TL, U.K.
email: Mark.Birkinshaw@bristol.ac.uk

²HH Wills Physics Laboratory, University of Bristol,
Tyndall Avenue, Bristol BS8 1TL, U.K.
email: J.Rawes@bristol.ac.uk

³HH Wills Physics Laboratory, University of Bristol,
Tyndall Avenue, Bristol BS8 1TL, U.K.
email: D.Worrall@bristol.ac.uk

Abstract. Jets often display bends and knots at which the flows change character. Extreme distortions have implications for the nature of jet flows and their interactions. We present the results of three radio mapping campaigns. The distortion of 3CRR radio galaxy NGC 7385 is caused by a collision with a foreground magnetised gas cloud which causes Faraday rotation and free-free absorption, and is triggered into star formation. For NGC 6109 the distortion is more extreme, creating a ring-shaped structure, but no deflector can be identified in cold or hot gas. Similar distortions in NGC 7016 are apparently associated with an X-ray gas cavity, and the adjacent NGC 7018 shows filaments drawn out beyond 100 kpc. Encounters with substructures in low-density, magnetised, intergalactic gas are likely causes of many of these features.

Keywords. Galaxies:active, galaxies:jets, radio continuum:galaxies, intergalactic medium

1. NGC 7385

NGC 7385 is radio-bright and a member of the complete 3CRR sample (Laing, Riley & Longair 1983) despite failing to be in the 3C catalogue because of its low redshift ($z = 0.0243$) and consequent large angular size. In low-resolution radio maps (e.g., Schilizzi & Ekers 1975) NGC 7385 appears as a radio trail source, with two distinct tails appearing about 300 kpc southwest of the core. The higher-resolution study by Simkin & Ekers (1979) found that the northeastern side of the source encounters an optically-bright, line-emitting cloud about 10 kpc from the nucleus of NGC 7385. The radio structure seems to disrupt at this point.

We have undertaken new radio, optical, and X-ray imaging of NGC 7385. An L-band radio map constructed from archival VLA data is shown in Fig. 1 superimposed on a galaxy-subtracted HST image (Rawes, Worrall & Birkinshaw 2015). The main jet extends to the southwest and is seen in the optical and X-ray in its inner regions. The wide bandwidth of our new data (Rawes, Birkinshaw & Worrall 2018b), allows spectral indices and Faraday rotation to be mapped at high angular resolution. Prominent features are associated with the gas cloud, showing that it lies on the near side of the counter-jet plume. The free-free optical depth and rotation measure through the cloud can be reconciled with a gas density of about 5 cm^{-3} and a magnetic field of order $1 \mu\text{G}$ provided that the cloud is strongly clumped.

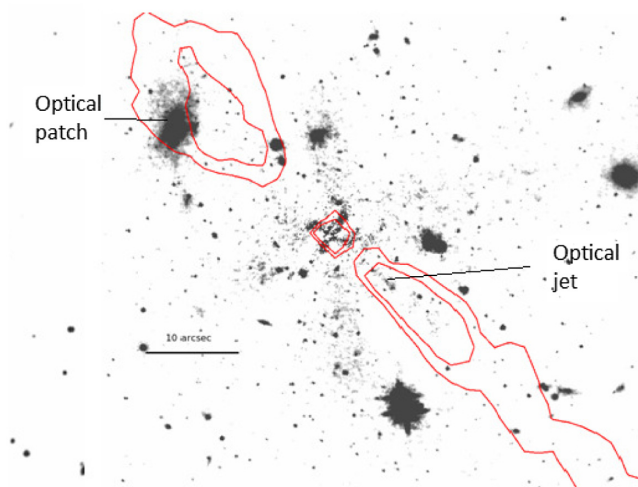


Figure 1. The centre of NGC 7385. At $z = 0.0243$ 10 arcsec corresponds to a projected scale of 4.9 kpc. Galaxy-subtracted HST F160W image with superimposed radio contours, from [Rawes, Worrall & Birkinshaw \(2015\)](#). An optical/X-ray jet extends southwest from the core. To the northeast the counter-jet is deflected and disrupted by the optical patch of [Simkin & Ekers \(1979\)](#), but retains enough integrity to flow back behind the main jet. We detect free-free absorption and Faraday rotation from the optical patch ([Rawes, Birkinshaw & Worrall 2018b](#)).

The strength of the cloud/counter-jet interaction causes the flow to turn through about 180 degrees, with the expanded, post-encounter, flow running back almost along the projected main jet, so that low-resolution maps show only a one-sided flow until different environmental conditions cause the projected structure to separate into two tails. This is likely due to gas flows and substructures on 100-kpc scales in the intergalactic medium of Zwicky cluster Zw 2247.3+1107, of which NGC 7385 is a member.

A high signal/noise IFU study of the cloud interaction might provide information about the momentum flux down the jet, and so potentially the jet composition, in the same way as has been possible for other jet/cloud interactions (e.g., PKS 2152-699; [Worrall *et al.* 2012](#), [Smith *et al.* 2018](#)). While such interactions are rare, they can provide the kinematic information that cannot be obtained from jet synchrotron (or synchrotron plus inverse-Compton) emission alone.

2. NGC 6109

NGC 6109, another neglected member of the 3CRR sample, exhibits a striking example of a radio ring. This low-redshift ($z = 0.0296$) galaxy appears, at low angular resolution, to be a radio trail source. [O’Dea & Owen \(1985\)](#) remarked that the source exhibited a small circular component to one side of the core, and a long tail to the other, and noted that this might indicate that the jet on one side was stopped by external gas, to create an FR II-like lobe, while it was drawn out into a long tail on the other.

Our high-resolution radio map ([Fig. 2](#)), shows that the southeastern feature is not a lobe but a circular loop ([Rawes, Birkinshaw & Worrall 2018a](#)). No excess or deficit of X-ray emission is seen in the neighbourhood of the loop, and there is no optical or infra-red emission, so the mechanism causing the loop is not like the interaction in NGC 7385.

The brightness contrast between the jet and counter-jet on sub-kpc scales can be interpreted in terms of a relativistic Doppler factor that associates the loop with the jet brightening 12-24 arcsec northwest of the core, so that both could arise from a single event in the AGN. However, relativistic flow and simple precession models cannot explain

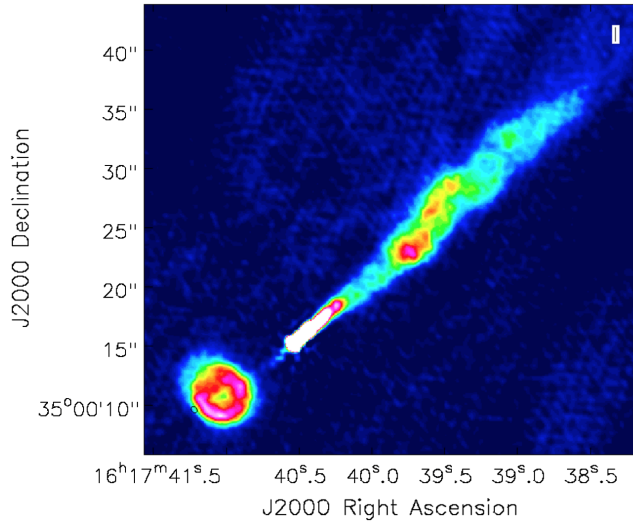


Figure 2. The centre of NGC 6109. At $z = 0.0296$ 5 arcsec corresponds to a projected scale of 3.0 kpc. S-band radio surface brightness image from Rawes, Birkinshaw & Worrall (2018a). The main jet extends northwest of the core for about 5 arcsec before fading, and then re-brightening in a less collinear structure 12–24 arcsec from the core. The counter-jet is faintly detected to about 5 arcsec, then develops a bright loop structure with radius 5 arcsec that lies outside the flattened X-ray emitting atmosphere detected by *Chandra*.

the structure: there must be asymmetrical acceleration/deceleration of the jet/counter-jet flow by the external medium. Although *Chandra* imaging shows little structured gas in the neighbourhood of NGC 6109, the galaxy is embedded in the large-scale atmosphere of a poor cluster, and our new polarisation data shows a Faraday rotation feature across the loop that could suggest interaction with a magnetic substructure such as a galactic wake in the intracluster medium.

3. Abell 3744

NGC 7016 and 7018 lie in Abell 3744, a moderately rich ($kT \approx 3$ keV) cluster of galaxies at $z = 0.0381$. Both galaxies host bright radio sources. The heating effects of the sources should combine to cause significant changes in the intracluster medium. Strong temperature and density structures are, indeed, seen across the cluster though these may be a consequence of a merger (Worrall & Birkinshaw 2014). Both radio sources are highly distorted (Cameron 1988; Bicknell, Cameron & Gingold 1990; Fig. 3), confirming that their interactions with the intracluster medium are strong.

The brightest parts of NGC 7018 show it to be of FR II character, with prominent hot spots at the ends of the lobes, a compact core, and a jet extending from the core towards the NE hot spot. Faint filamentary structures extend from both lobes and lie around a prominent cavity in the cluster's X-ray emission (Worrall & Birkinshaw 2014). One filament, < 2 kpc in diameter, can be traced to > 150 kpc, where it seems to end in a faint radio source that might have punctured one lobe of NGC 7018 (Birkinshaw, Worrall & Rawes 2018).

NGC 7016 shows a bent, twin-sided, FRI structure in its inner parts. However, to the north the jet appears to reverse direction and expand, and then to create a radio ring (Worrall & Birkinshaw 2014), before disrupting into a faint array of radio filaments and flowing back parallel to the southern jet (Birkinshaw, Worrall & Rawes 2018). This is seen as a broad structure around the jet in low-resolution maps. The sequence of structures,

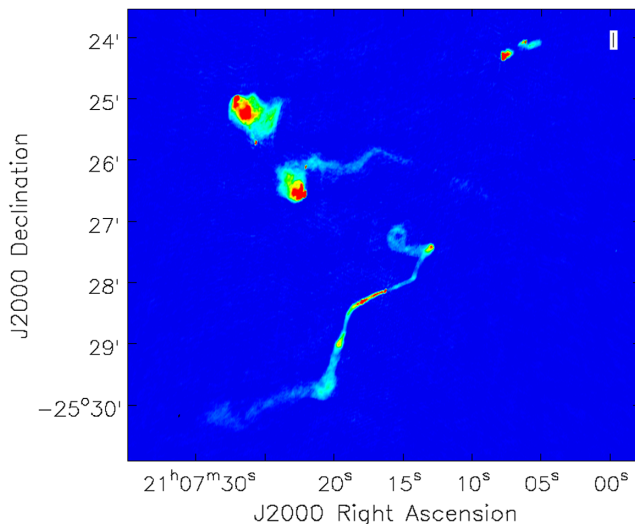


Figure 3. Abell 3744 from Birkinshaw, Worrall & Rawes (2018). At $z = 0.0381$ 5 arcmin corresponds to a projected scale of 230 kpc. The image is dominated by NGC 7016 to the southwest and NGC 7018 to the northeast. An unusual (background?) radio source lies to the northeast.

with the ring downstream of the reversal, might indicate that the reversal is a younger version of the ring, and will develop into a full ring in a few Myr.

The X-ray cavity would collapse rapidly without internal pressure support. This can arise from the repository of electrons within the cavity that produce the diffuse radio emission mapped by Cameron (1988). The irregular X-ray structure suggests that Abell 3744 is dynamically young (Worrall & Birkinshaw 2014), so that rapid gas motions are likely and could cause some of the radio distortions, though the ring and reversal features seem surprisingly compact unless they are short-lived.

4. Generalisation

The extreme distortions in Figs. 1–3 were detected in arcsec-resolution, high dynamic-range, low-frequency mapping. High resolution is necessary, even at low redshift, to detect the kpc-scale substructures we are reporting. Extreme distortions cannot be rare, since we have two examples (NGC 6109 and NGC 7385) in the low-redshift 3CRR sample of only 35 radio galaxies, so the SKA should find many such structures in the future, as its sub-arcsec capabilities reveal them at redshifts beyond $z = 1$.

While some distortions arise from interactions with optically-emitting gas, where there is the potential for obtaining important dynamical information about the jet flows (e.g., NGC 7385, PKS 2152-699), sometimes there is no clear deflecting gas (NGC 7016, NGC 6109). The evolution of dynamical activity in clusters and groups around low-thrust radio sources could be studied by future radio mapping.

References

- Bicknell, G. V., Cameron, R. A., & Gingold, R. A. 1990, *ApJ*, 357, 373
 Birkinshaw, M., Worrall, D. M., & Rawes, J. 2018, in preparation
 Cameron, R. A. 1988, PhD thesis, ANU
 Laing, R. A., Riley, J. M., & Longair, M. S. 1979, *MNRAS*, 204, 151
 O’Dea, C., & Owen, F. 1985, *AJ*, 90, 927
 Rawes, J., Worrall, D. M., & Birkinshaw, M. 2015, *MNRAS*, 452, 3064
 Rawes, J., Birkinshaw, M., & Worrall, D. M. 2018a, *MNRAS*, 480, 3644

- Rawes, J., Birkinshaw, M., & Worrall, D. M. 2018b, *MNRAS*, in preparation
- Schilizzi, R., & Ekers, R. 1975, *A&A*, 40, 221
- Simkin, S. M., & Ekers, R. D. 1979, *AJ*, 84, 56
- Smith, D. P., Young, A. J., Worrall, D. M. & Birkinshaw, M. 2018, *MNRAS*, submitted
- Worrall, D. M., & Birkinshaw, M. 2014, *ApJ*, 784, 36
- Worrall, D. M., Birkinshaw, M., Young, A. J, *et al.* 2012, *MNRAS*, 424, 1346